Yttrium Doped TiO2 Thin Film for Gas Sensing Application Prepared by Spin Coating Method

M Abdul Kaiyum (kaiyum@gce.ruet.ac.bd)
Rajshahi University of Engineering and Technology https://orcid.org/0000-0001-9160-304X
Naim Ahmed
Dept. of Glass & Ceramic Engineering (GCE)
Arif Alam
Dept. of Glass & Ceramic Engineering (GCE)
M Shamimur Rahman
Dept. of Glass & Ceramic Engineering (GCE)

Research Article

Keywords: thin film, crystal structure, surface roughness, extrinsic impurities

Posted Date: November 18th, 2020

DOI: https://doi.org/10.21203/rs.3.rs-106302/v1

Yttrium Doped TiO_2 Thin Film for Gas sensing application Prepared by Spin Coating Method

M Abdul Kaiyum*[1], Naim Ahmed[1], Arif Alam[1], M Shamimur Rahman[1]

*kaiyum@gce.ruet.ac.bd

[1]Department of Glass & Ceramic Engineering (GCE), Rajshahi University of Engineering & Technology (RUET), Rajshahi-6204, Bangladesh

Abstract: Yttrium (Y) doped and pure Titanium Di-oxide (TiO_2) thin films were prepared by using spin coater. The coater was set up in laboratory with low cost investment. The films were calcined at 450°C for 1 hour. For characterization, Scanning Electron Microscopy (SEM), Energy Dispersive X-Ray Analysis (EDX), X-ray diffraction (XRD), X-ray photoelectron spectroscopy (XPS), Atomic Force Microscopy (AFM) were carried out. LCR Bridge - GW Instek LCR-821 was used for gas sensing applications. XPS showed that the change of electronic structure due to Y doping. SEM and AFM analysis were carried out to determine the surface morphology of the films. Yttrium (Y) decreased the crystallite size of the films and increased the surface roughness and porosity value, which was very good for many sensing applications. Gas sensing property of the deposited films were improved by the incorporation of yttrium impurities and the sensing property improved almost two times than pure TiO_2 thin film. Different researches have been done their research related to this topic but no one researchers provide a precise explanation of their results, authors of this research have tried to do that. Moreover the films were prepared by a simple spin coater to reduce the production cost also.

Keywords: thin film, crystal structure, surface roughness, extrinsic impurities.

1. Introduction

Our climate is getting poisoned by poisonous fumes day after day. It emerged from the functions of factories, internal combustion engines, etc. To control the air quality, Waste products should be controlled. If it is possible to control the pollution, than the toxicity in air will be decreased [1,2]. The universe is surrounded by dangerous and distinct poisonous gases, which can drive us to death in the future. We have a duty to maintain such gases in the environment.

A large number of workers died every year because of toxic gases who worked in mining plant, coal plant, septic tank and drainage system. The number of people who died while cleaning sewers and septic tanks in India increased by almost 62%, from 68 in 2018 to 110 in 2019[3]. At least 592 workers were died across Bangladesh in 2018 [4]. So it is our responsibility to save the worker from toxic gases. In the market, gas sensors based huge technologies are available. Much effort has been made in recent years to boost the Gas sensors selectivity and responsiveness.
TiO_2 has received attention and is given prime importance in gas sensor industry [5]. TiO_2 Chemical stability, non-toxic condition, low cost, production versatility, and ease of use of TiO_2 attract researchers [6]. All over the world a lot of techniques are developed to fabricate TiO_2 thin films as like as PLD (Pulsed Laser Deposition), Sol-Gel dip coating, CVD (Chemical Vapor Deposition), Evaporation, Sputtering etc. [7,8]. Spin coating technique has been used for its good quality film [8], the short coating time and high resist film [9], and a homemade spin coater can reduce the initial cost also.TiO_2 thin films can be obtained using the sol-gel technique, which is a reliable and low-cost chemical route too but the spin coating method is widely used for the deposition of materials [10].

TiO_2 is an n-type semiconductor with low conductivity [11]. There was a lot of effort there has been given for the doping of TiO_2 with metal atoms, where the electrons are transferred from one atom to another atom, allowing creatures to the total electrical charge to be generated [12]. Transition metal ions like Iron (Fe), Chromium (Cr), Cobalt (Co), yttrium (Y) etc. can be used as dopant in TiO_2 thin films [13].

The misfit strain energy formed from of Y^{+3} (1.015Å) and Ti^{+4} (0.68Å) in yttrium doped TiO_2 thin film [14]. In this research, Yttrium doped TiO_2 thin films were fabricated using a simple spin coater and investigated gas sensing properties, crystal structure, microstructure and optical properties. Because of size differences of Y^{3+} and Ti^{4+}, substitution doping will be happened. The aim of this work was to find the optimum Yttrium doping concentration to enhance gas sensing properties and to find the structural, morphological and electron transportation ability of TiO_2 thin films on a glass substrate.

2. Methodology

Titanium isopropoxide (TTIP) (Sigma-Aldrich, 97%) was as a precursor of TiO_2, and ethanol (C_2H_5OH) was used as a solvent. The secondary solution of yttrium (III) nitrate hexahydrate ($Y(NO_3)_3.6H_2O$) was dopant precursor for Y^{+3}. The precursor and dopant precursor were mixed in different ratio to form 0%, 1%, 2%, and 3% Y doped TiO_2 thin film.

A simple spin coater was made in lab (Fig.S1), from locally available components. The thin films were prepared by using the homemade spin coater. The slide were spun in air at 2000 rpm for 1 minute and annealed at 450°C for 60 minutes.The XRD patterns of un-doped and Y doped TiO_2 thin films were analyzed by 'Bruker, D8 Advanced' machine, where the wavelength of X-ray radiation was 1.5406 Å for CuKα. In this research, the films were characterized by SEM (ZEISS). The parameters of the SEM machine were fixed as: EHT- 20.00 KV; WD - 6.5; Mag.; 20 KX. For determining the surface roughness values, AFM analysis was carried out. XEI-70 AFM Software was used to analyses the images. XPS was used to find out to determine the position of dopant atom. Finally gas sensing properties were measured by using LCR Bridge-GW Instek LCR-82, where different gases (NH_3, C_3H_8O, CO and CO_2) were used for sensing application.

3. Results and Discussion

3.1 XRD analysis

Structural characterization of undoped and yttrium (Y) doped TiO_2 was obtained by X-ray diffraction. The stabilized Anatase tetragonal phase was found and dominant peaks were at plane angle 2θ=25.85°, 38.64° and 48.14° and the (hkl) coordinates were (101), (112), (200) which corresponded to ICSD file no. 98-015-4601, illustrated in Fig.1.

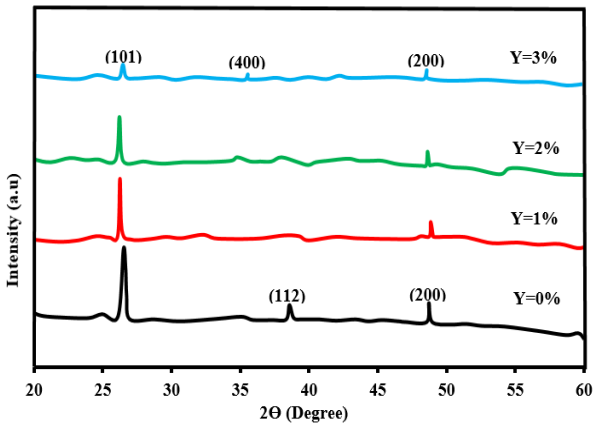

Fig.1: X-ray diffraction patterns of pure and Y:TiO_2 thin films

From that peak analysis it was found that the films were polycrystalline with tetragonal crystal structure, because nucleation sites started during sintering and films became more crystalline [15]. The crystallinity of the film influenced the transport properties of the photo generated electrons and holes to the film surface [16]. With increasing the dopant concentration, the peaks became wider and gradually removed. At Y=3% the additional peak (400) was raised which indicated the alteration of plan. The preferred orientation of the film was determined in texture coefficient (T_c) relation, which is shown in the following Eq. (1) [17].

$$T_c\,(hkl) = \frac{\frac{I}{I_0}}{\frac{1}{n}\sum_{i=1}\frac{I}{I_0}} \qquad (1)$$

Where, where I was measured intensity, I_o was JCPDS intensity and n was the reflection number.From that calculation (101) and (200) plan was indicated as preferred plan for TiO_2 thin films.

An important scenario was observed that Y concentration shifted the peak (101) from right to left. The intensity of (101) diffraction peak decreased with increasing Y doping. The ionic radius of Y^{3+} was larger than Ti^{4+}. Hence, Ti^{4+} was replaced by Y^{3+}. There was on peak for Y_2O_3 which indicated that the proper doping process.Y^{3+} ions were not segregated to form Y_2O_3 at Y=0%, Y=1% and Y=2%, but at Y=3% a small amount of segregation was observed in morphological analysis (AFM and SEM). Due to doping of yttrium different structural changes were found. Those were calculated by using different techniques, among of them Scherrer formula was used to calculate lattice parameters, shown in Table 1. Lattice parameters were calculated by using the Scherrer Eq. (2) [18].

$$\mathbf{d=\left(\frac{k\lambda}{\beta Cos\theta}\right)} \qquad \mathbf{(2)}$$

Where, λ (0.154 nm) was the wavelength of X-rays, θ diffraction angle, and $k = 0.9$, β was full-width half maximum intensity (FWHM) of the diffraction peak.

The crystallite size decreased with increasing dopant. Crystallite size, lattice strain, and dislocation density are shown in Table S1. Due to Y doping, lattice parameters a, b and c axis, were changed. So, crystal structure changed, and derived a structural transformation (Tetragonal to orthorhombic) or (Anatase to Pseudobrookite). For 3%Y doping orthorhombic structure was formed i.e. Pseudobrookite but some Anatase also existed at that point shown in Table 1.

Table 1: Parameters of structural characterization

Sample%	Peak position (2Θ)	Intensity (Cts.)	Crystallite size, d(nm)	Dislocation density, Đ	Lattice strain, η	Stress, σ (GPa)	Lattice parameters		Crystal structure	Name of structure
							a (Å)	c (Å)		
Y=0	25.85	152	41.09	0.59	3.37	0.91	3.781	9.592	Tetragonal	Anatase
Y=1	25.45	132	31.91	0.98	4.34	-1.37	3.784	9.763	Tetragonal	Anatase
Y=2	25.11	119	25.55	1.53	5.42	-2.54	3.801	9.881	Tetragonal	Anatase
Y=3	25.39	108	25.95	1.48	5.34	-2.65	3.800	9.995	Orthombic	Anatase+ Pseudobrookite

Using the following Eq. (3), the lattice constants were determined [16].

$$\frac{1}{d^2} = \frac{h^2+k^2}{a^2} + \frac{l^2}{c^2} \qquad (3)$$

The stability of the films depends on the stresses of the film. The stress (σ) of the prepared thin films were calculated using Eq. (4) [19].

$$\sigma = \frac{2C_{13}^2 - C_{33}(C_{11}+C_{12})}{2C_{13}} \times \frac{(C-C_0)}{C_0} \qquad (4)$$

Where, C_{11}= 208.8 GPa, C_{33}=213.8 GPa, C_{12}=119.7 GPa and C_{13}=104.2 GPa. The resultant stresses are shown in Table 1. From the XRD analysis, in terms of crystallite size, it is possible that Y^{3+}ion doping promoted the anisotropic adsorption of ions on (101) planes of TiO_2, and thus enhanced the anisotropic growth of TiO_2 crystallites [20].

However, Y=1%, Y=2%, and Y=3% samples showed an increase in lattice parameters and decreased crystallite size which can be related to high lattice distortion in the crystallization process [21]. It was found that variation in ionic radius of Y and Ti changed the axis values and a helped to separate the electrons or removed the possibility of recombination of hole and electron pairs [22]. As a result the sensitivity of thin films were increased.

3.2 Surface morphology

In this research, SEM images of the doped and undoped TiO_2 thin films are given in Fig.2.

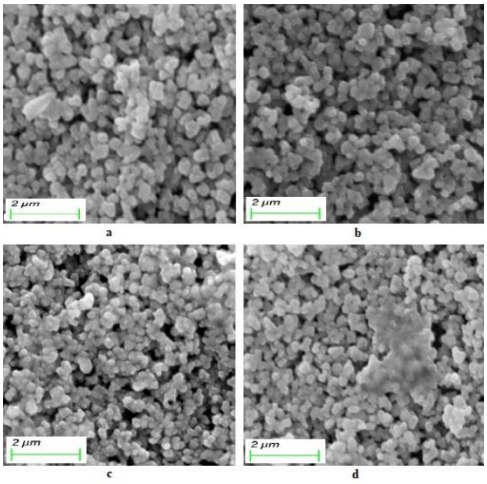

Fig.2: SEM images of TiO_2 thin films, (a) Pure TiO_2; (b) 1%Y:TiO_2; (c) 2%Y:TiO_2; (d) 3%Y:TiO_2.

It was found that the Y:TiO_2 films were porous as a result the reactive surface area of the films increased which was very important for gas sensing applications. The porosity of the films were increased with increasing the concentration of Y. at Y=2% highest amount of porosity was noticed. The pores were acted as conducting channel for gas sensing.

At Y=3% the porosity became decreased, it might be the effect of structural change which is shown in XRD analysis. The grain growth also happened in 3%Y:TiO_2 film (Fig.S2). The particles were in spherical in shape too. For determining the component, EDX & XPS were carried out (Fig.S3 and Fig.S4) of Y:TiO_2 film, which is shown in supplementary files . The element mapping established that the existence of Y in TiO_2 and $Y_2Ti_2O_7$was formed [24]. The surface roughness values of TiO_2 and grain growth values of the films were determined from the AFM image analysis. AFM morphological images are shown in Fig.3.

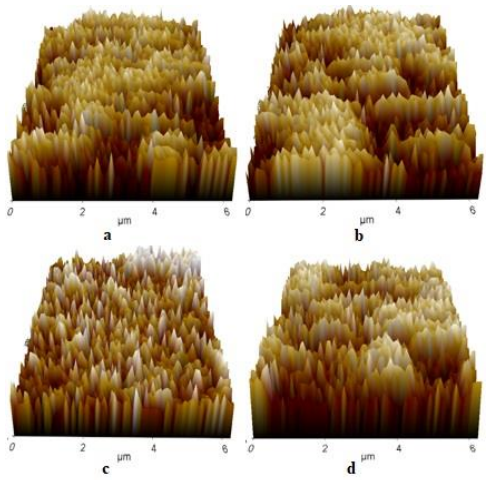

Fig.3: AFM images of TiO_2 thin films, (a) Pure TiO_2; (b) 1%Y:TiO_2; (c) 2%Y:TiO_2; (d) 3%Y:TiO_2.

The formation of Anatase TiO_2 crystals increased the surface roughness and developed pores [25]. It was found that the grain sizes increased with increasing the dopant concentration and Fig.3 indicated that maximum rough surface was found at 2%Y: TiO_2. The minimum grain size was found 35 nm, when Y=0%, and maximum grain size was 48 nm when Y=3%. The roughness was maximum (S_a=116.39) when Y=2%. At 3%Y:TiO_2, the grain became enlarged and the roughness became low (S_a=78.85), all other roughness values are shown in Table 2. So, the less amount of reactivity of sensing for gases was found.

Table 2: Surface properties of TiO_2 and Y:TiO_2

Sample %	Grain size (nm)	Roughness		
		S_a	S_q	S_z
Y=0	35	47.17	94.70	458.3
Y=1	42	56.40	103.33	644.6
Y=2	43	116.39	198.49	750.6
Y=3	48	78.85	110.04	622.56

3.3 Gas sensation

The operation temperature was 250^0C, which was fixed. The gas-sensing performance of the nanostructured thin films was tested using static gas-sensing system [26]. The reading was collected from the digital display and recorded before and after testing. The test was carried out by using NH_3, CO, CO_2, C_3H_8O and the concentration was varied from 100 to 900 ppm. The response (S) of the films to gas was calculated by using the following Eq. (5) [27].

$$S=\frac{R_0-R_G}{R_G} \qquad (5)$$

Where, R_0 was the resistance of air and R_G was the resistance of gas inside chamber. The sensing properties of any materials depends on crystallite size, reactive surface area, microstructure, structure, and grain sizes. At low temperature (<300ºC), oxygen was adsorbed on the oxide crystals surface as ions were formed by abstracting free electrons from the semiconductor solid, reducing the electrical conductivity[28].

A layer of oxygen ions that produced a repulsion force over the charge carriers inside the films. Then, in the middle of the crystals, the charge carriers were trapped and a leakage surface layer just below the crystal surface was formed. So, a potential barrier appears between the oxide crystals, causing an additional reduction of the electrical conductivity [29].

It was found that the response of films was increased with increasing concentration of NH_3. At 300 ppm, the response was highest and 400 ppm to 900 ppm the response became constant. The response also related to the concentration of Y. At Y=0% the response was lowest and maximum response was found at Y=2%, after that the response decreased at Y=3%. Based on that, the additive of yttrium improved their sensing performance by the way of high surface area to volume ratio [30]. In the exposure of NH_3, the gas reacted with the adsorbed oxygen, left free electrons and the formed ions kept free. The reaction can be represented as following Eq. (6) [31].

$$NH_3 + O_2 \longrightarrow NO + H_2O + e^- \qquad (6)$$

The responses of different gases are given in Fig.4. All the responses of NH_3 (a), CO (b), C_3H_8O (c), and CO_2 (d) showed the concentration effect of yttrium and gases. But the percentages of response of NH_3 was highest (a) and C_3H_8O was lowest (c).

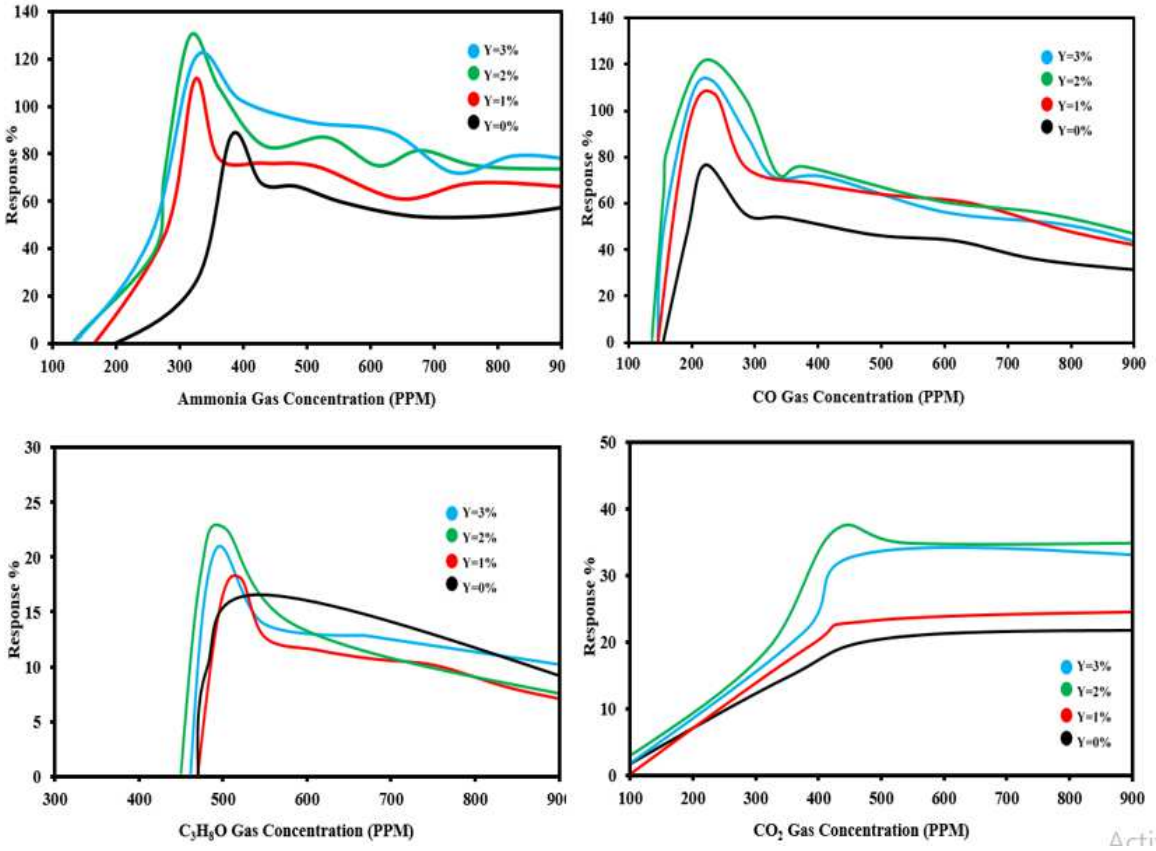

Fig.4: Response of different gases with different composition of thin films and concentrations of gases

The gases on the surface of the films conducted electrons. As a result the sensational properties were found. All the response percentages were found between 100 ppm to 200 ppm concentration, except C_3H_8O. The response percentages were increased with the increased of Yttrium (up to Y=2%), but at Y=3% the response became low but not less than 1%Y doped thin film. This statement was true for all kind of gases showed in the Fig.4. This was happened, because of grain growth, low porosity, low surface roughness, structural alteration and agglomeration of yttrium on the surfaces of the films at 3%Y:TiO_2.

4. Conclusion

TiO_2 and Y:TiO_2 thin films were successfully fabricated by using spin coating technique. The films were sensitive for NH_3, CO, CO_2 and C_3H_8O gases. The films showed maximum

sensitivity for 2%Y:TiO_2 composition. The crystallite sizes of the films were decreased with increasing the Y concentration. The sensitivity of the films depended on surface porosity and surface roughness. Yttrium doped TiO_2 thin films, fabricated by spin coating method can be used in ceramic sensors of gas sensing applications.

5. Acknowledgement

Authors of this work would like to thanks the department of Glass & Ceramic Engineering (GCE) for providing equipment facilities.

6. Supplementary materials

This paper contains supplementary material available online.

References

1. H. Tang, K. Prasad, R. Sanjinès, and F. Lévy, Sens. Actuators B 26–27, 71 1995".

2. E. Williams, Sens. Actuators B 57, 1. 1999".

3. The Hindus. New Delhi, India, February 11, 2020 22:55 IST.

4. https://www.thedailystar.net/city/news/592-killed-workplace-accidents-2018-1682341.

5. D. Mardare, N. Iftimie, D. Luca, TiO_2 thin films as sensing gas materials. J. Non.Cryst. Solids 354, 4396 (2008).

6. I. Vaiciulis, M. Girtan, A. Stanculescu, L. Leontie, F. Habel-hames, S. Antohe, On titanium oxide spray deposited thin ilms for solar cells applications. Proc. Rom. Acad. Ser. A 13(4), 335 (2012).

7. C. J. Brinker and M. S. Harrington, Sol–gel derived antireflective coatings for silicon, Solar Energy Mater. 5, 159(1981).https://doi.org/10.1016/0165-1633(81)90027-7.

8. Hanaor, D., Trianni, Morphology G. And and photo catalytic Sorrell, activity C. of highly oriented mixed phase titanium dioxide thin film", CC (2011)-3664.205 (12). https://doi/10.1016/j.surfcoat.2011.01.007.

9. Trianni, G. and Morphology Sorrell, and photo catalytic C. activity (2011), of highly "oriented Mixed phase titanium dioxide thin film", CC (2011). 205(12).

10. J.A.Byrne, et al., Titanium Dioxide Nanostructured Coatings: Application in Photo catalysis and Sensors, 2006, vol. 1, pp. 72-75.

11. D. Mahesh and J. Rajesh, TiO_2 Microstructure, Fabrication of thin Film Solar Cells and Introduction to Dye Sensitized Solar Cells, Res. J. Recent Sci, 2003, 2,25-29.
12. A. Di Paola, S. Ikeda, G. Marc, B. Ohtani and L. Palmisano, Transition metal doped TiO_2: Physical properties and photo catalytic behavior, Int. J.Photo energy, 2001, 3,171,176.
13. K. T. Ranjit and B. Viswanathan, Synthesis and characterization and photo catalytic properties of Iron-doped TiO_2 catalysts, J. Photo chem. Photo biol. A: Chem. 108, 79(1997). https://doi.org/10.1016/S1010-6030(97)00005-1.
14. M. I. Litter and J. A. Navio, Photo catalytic properties of irondoped titania semiconductors, J. Photochem. Photobiol. A: Chem. 98, 171 (1996).https://doi.org/10.1016/101-6030(96)0443-2.
15. Ritala, M.; Leskelä, M.; Niinistö, L.; Haussalo, P.; Niinist, L. Titanium Isopropoxide as a Precursor in Atomic Layer Epitaxy of Titanium Dioxide Thin Films. Chem. Mater. 1993, 5, 1174-1181.
16. C. Paper, et al. , Eff ects of Al doping on structural, morphology,electrical and optical properties of TiO_2 thin film, 2017, DOI:10.1063/1.4968383.
17. R. Suresha, V. Ponnuswamy, R. Mariappan, Nanostructured cerium oxide thin films by nebulized spray pyrolysis (NSP) technique: Impact of surfactants on the structural, optical and compositional properties. Ceram. Int. 40, 13515 (2014).
18. J.W. Zhang, G. He, T.S. Li, M. Liu, X.S. Chen, M. Liu, Z.Q. Sun, Modulation of microstructure and optical properties of Mo-doped ZnO thin films by substrate temperature, Mater. Res. Bull. 65 (2015) 7–13.
19. L. B. Freund and S. Suresh, Thin Film Materials: Stress, Defect Formation and Surface Evolution, Cambridge University Press, 2004.
20. Li Y M, Guo Y, Li Y H and Zhou X F 2016 Fabrication of Cd-doped TiO_2 nanorod arrays and photovoltaic property in perovskite solar cell Electrochim. Acta 200 29-36.
21. D 'Souza L P, Shwetharani R, Amoli V, Fernando C A N, Sinha A K and Balakrishna R G 2016 Photoexcitation of neodymium doped TiO2 for improved performance in dye-sensitized solar cells Mater. Design 104 346-54.
22. W. Zhang, K. Wang, S. Zhu, Y. Li, F. Wang and H. He, Yttrium-doped TiO_2 films prepared by means of DC reactive magnetron sputtering, Chem. Eng. J, 2009, 155, 83-87; X. Pei, J. Chen and H. He, Effects of Al doping on properties of x Al3%, In-TiO2 photocatalyst prepared by a sol-gel method, Mater. Sci. Semicond. Process., 2015, 3, 24-30.

23. Zhang H.R, Tana K.Q, Zheng H.W, Gua Y.Z and Zhang WF 2011 Preparation, characterization and photocatalytic activity of TiO2 codoped with yttrium and nitrogen, Mater. Chem. Phys. 125 156-60.

24. Q. Wang, G. Lian, and E. C. Dickey, "Grain boundary segregation in yttrium-doped polycrystalline TiO_2," vol. 52, pp. 809-820, 2004, doi: 10.1016/j.actamat.2003.10.016.

25. W. Zhang, K. Wang, S. Zhu, Y. Li, F. Wang, and H. He, "Yttrium-doped TiO_2 films prepared by means of DC reactive magnetron sputtering," vol. 155, pp. 83-87, 2009, doi: 10.1016/j. cej.20096.039.

26. G. E. Patil, D. D. Kajale, D. N. Chavan, N. K. Pawar, V. B. Gaikwad, G. H. Jain," Spray Pyrolysis polycrystalline Tin Oxide Thin film as Hydrogen Sensor", Sensor and tranducer,12, (2010) pp.70-79.

27. A.A. Haidrya, J. Puskelova, T. Plecenik, P. Durina, J. Gregus, M. Truchly, T. Roch, M. Zahoran, M. Vargova, P. Kus, A. Ple-cenik, G. Plesch, Characterization and hydrogen gas sensing properties of TiO2 thin ilms prepared by sol–gel method. Appl. Surf. Sci. 259, 270 (2012).

28. S. B. Patil and R. H. Bari, "Sprayed nanostructured TiO_2 thin films and its application for gas sensor," vol. 9, no. 8, pp. 33-45.

29. L.A. Patil, A. R. Bari, M.D. Shinde, Vinita Deo, D.P. Amalnerkar, "Synthesis of ZnO Nanocrystalline Powder from Ultrasonic Atomization Technique, Characterization, and its Application in Gas Sensing", IEEE Sensors, 11(2011) pp.939-946.

30. C. Garzella, E. Comini, E. Tempesti, C. Frigeri, G. Sberveglieri, TiO_2 thin ilms by a novel sol gel processing for gas sensor applications. Sens Actuators B 68, 189 (2000).

31. V. G. Krishnan and P. E. V Ganesan, "Surface characterization and gas sensing performance of yttrium doped-TiO_2 nanofilms prepared by automated nebulizer spray pyrolysis (ANSP)," J. Mater. Sci. Mater. Electron., vol. 0, no. 0, p. 0, 2017, doi: 10.1007/s10854-017-7928-9.

Figures

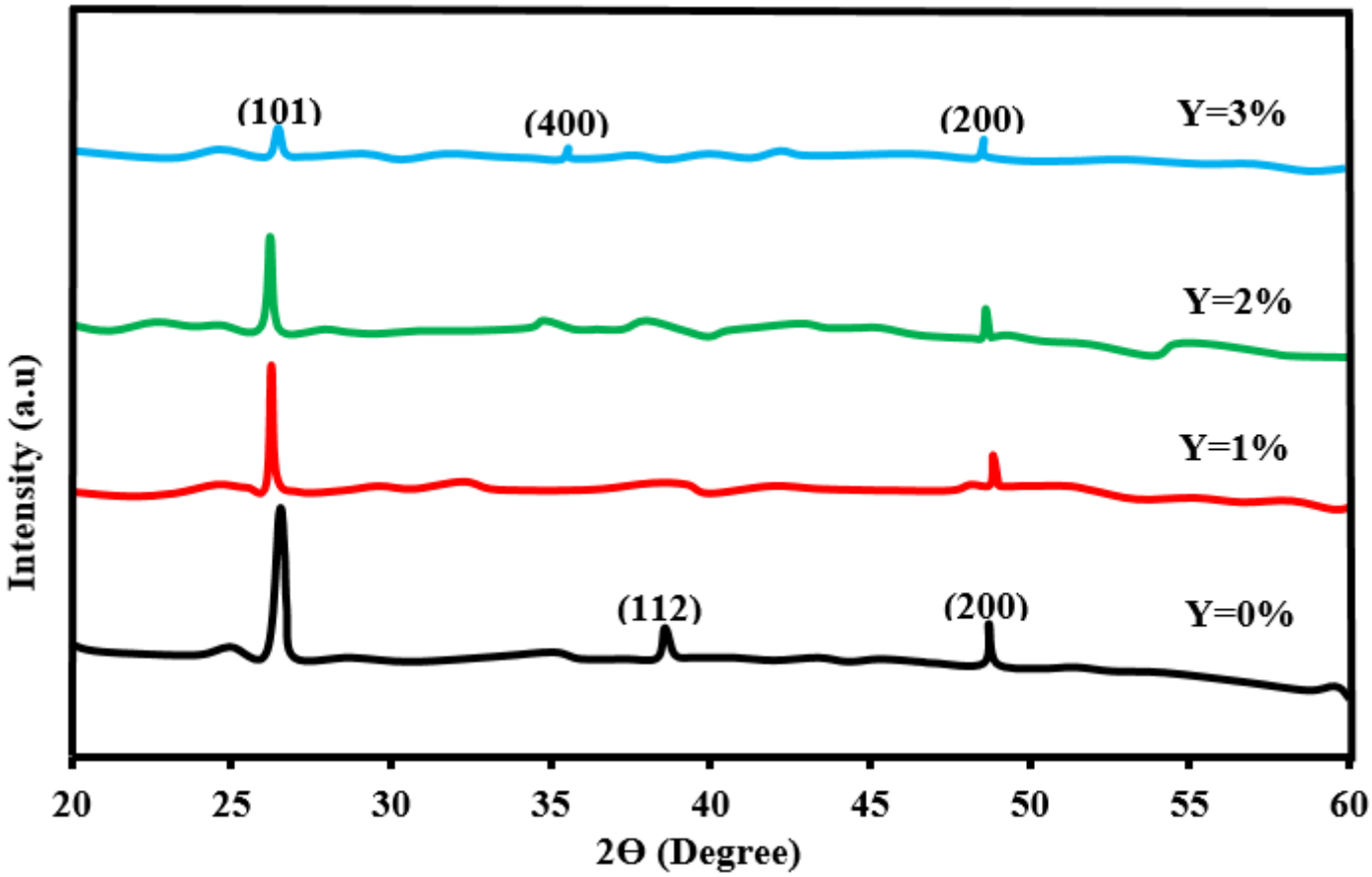

Figure 1

X-ray diffraction patterns of pure and Y:TiO2 thin films

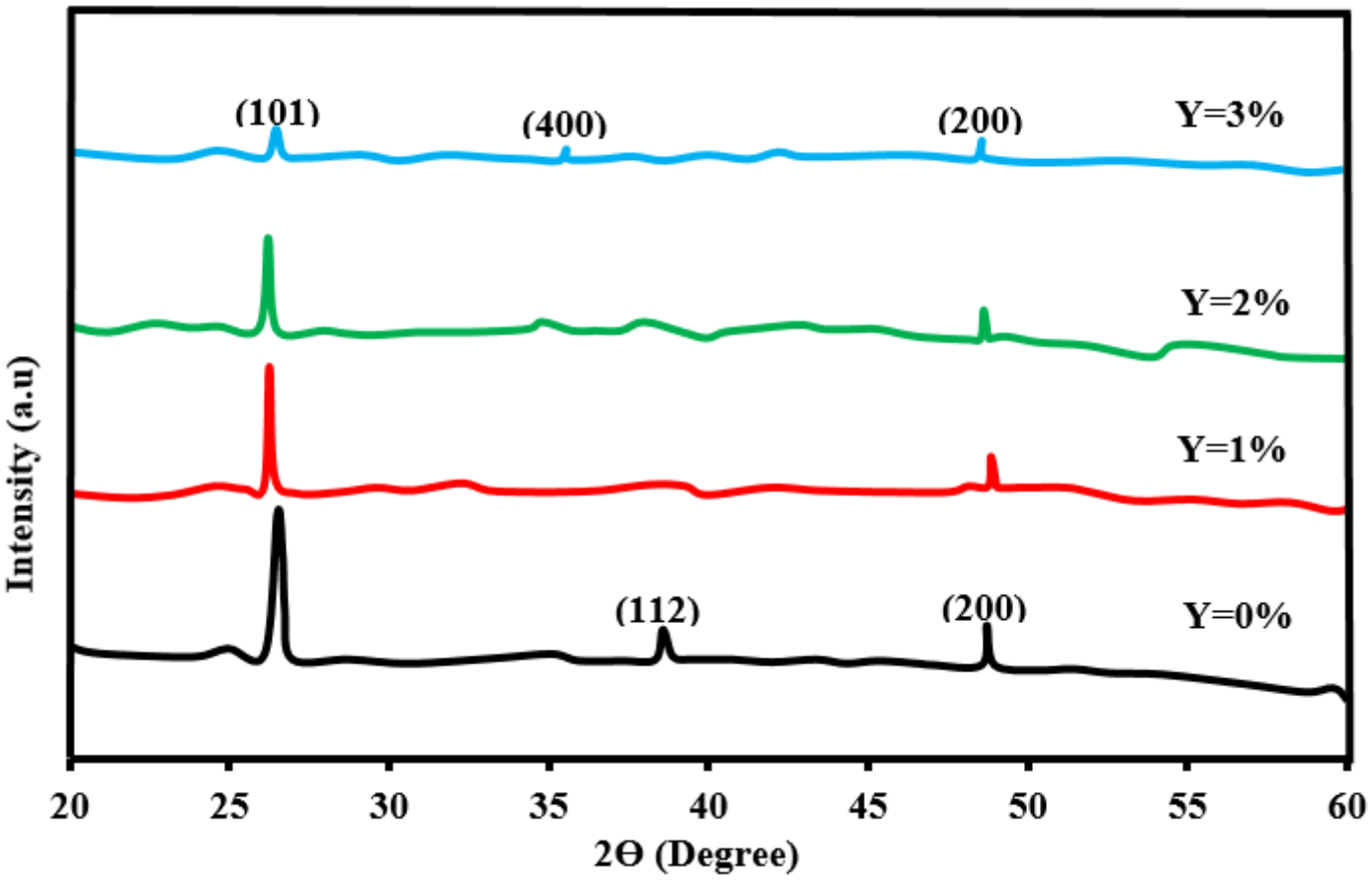

Figure 1

X-ray diffraction patterns of pure and Y:TiO2 thin films

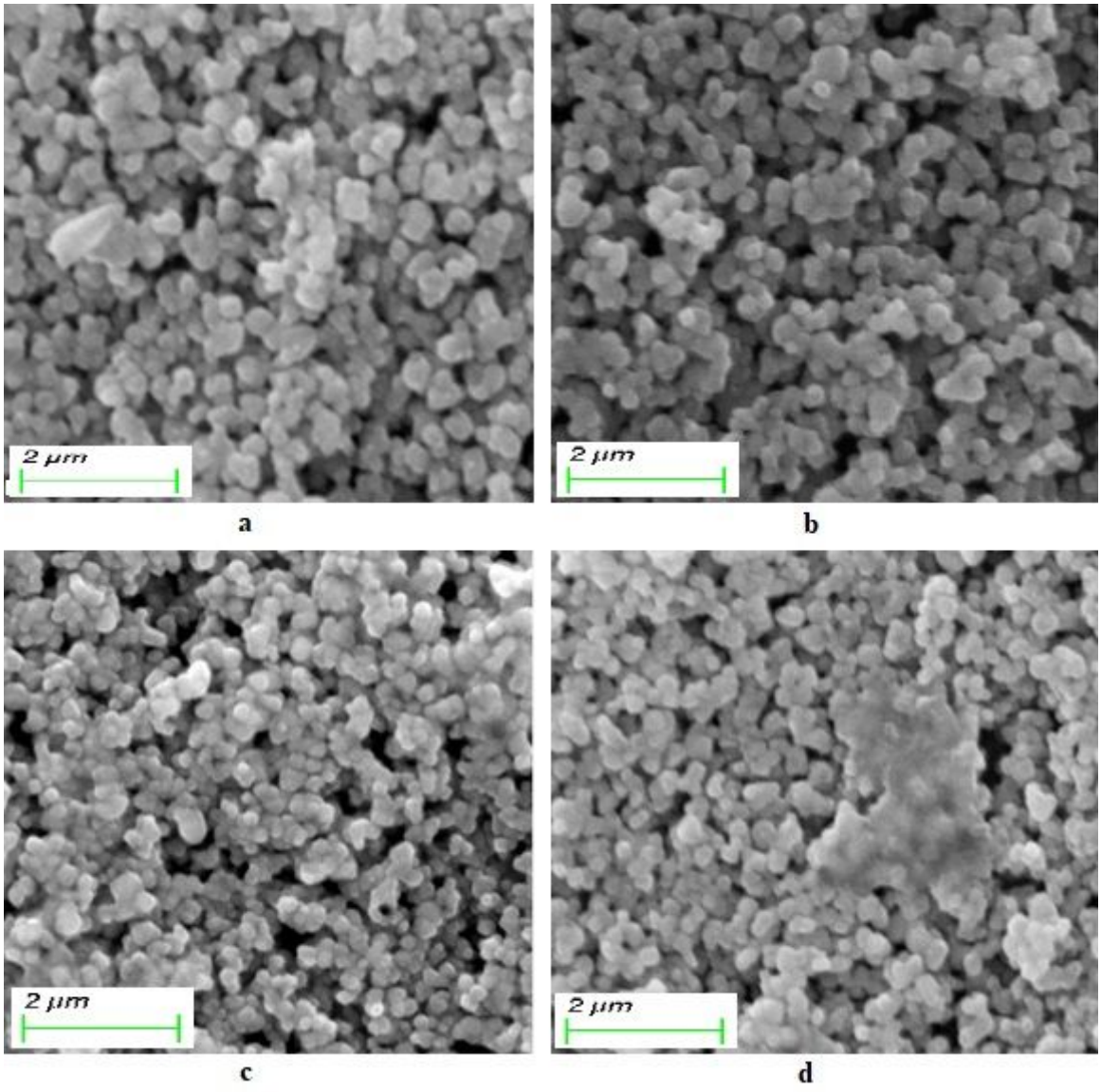

Figure 2

SEM images of TiO2 thin films, (a) Pure TiO2; (b) 1%Y:TiO2; (c) 2%Y:TiO2; (d) 3%Y:TiO2.

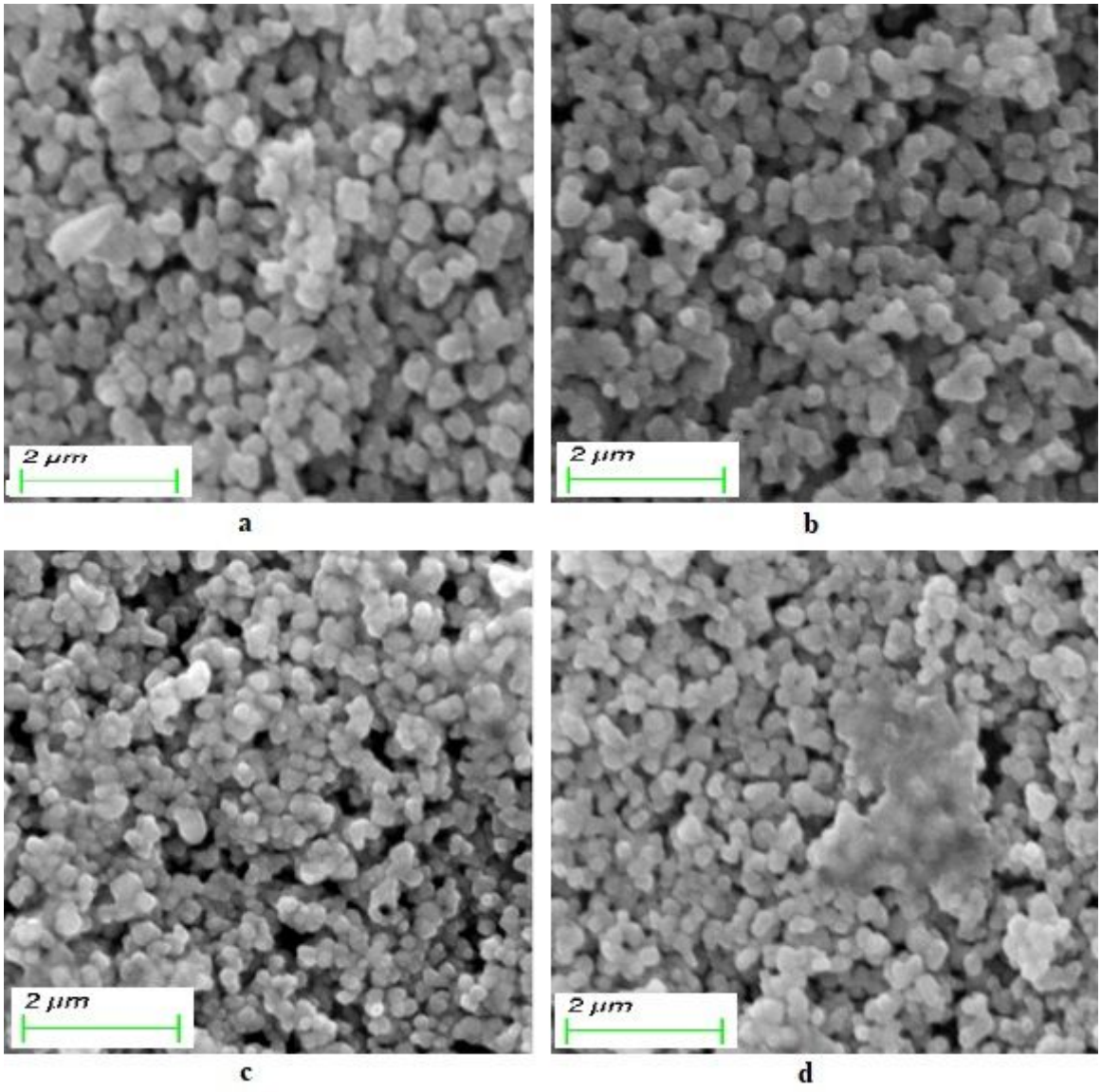

Figure 2

SEM images of TiO2 thin films, (a) Pure TiO2; (b) 1%Y:TiO2; (c) 2%Y:TiO2; (d) 3%Y:TiO2.

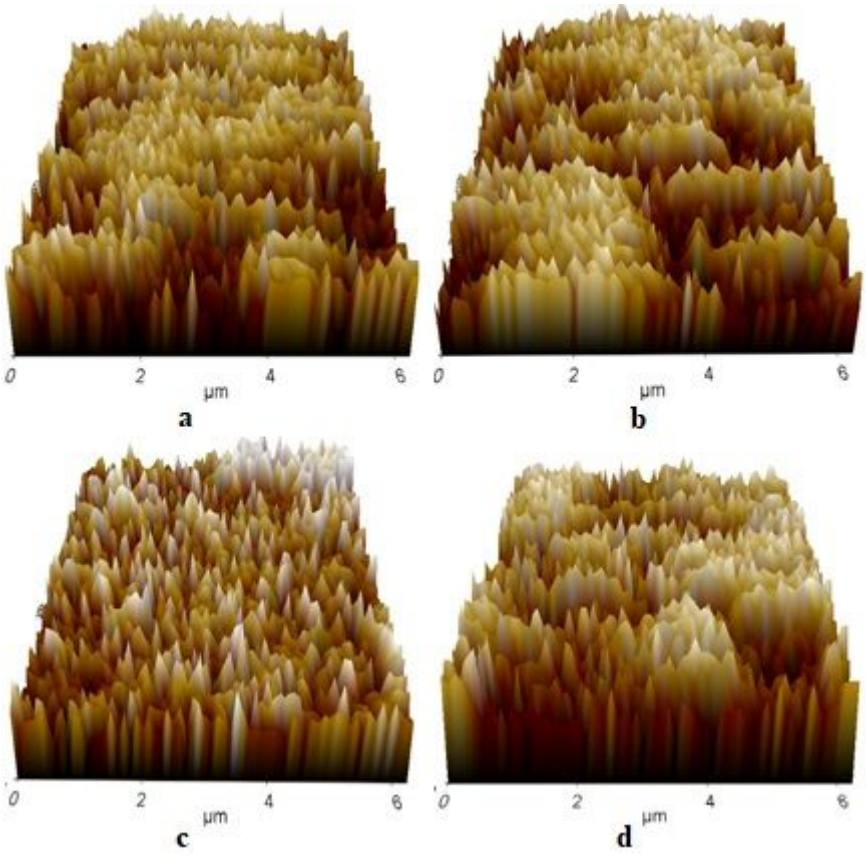

Figure 3

AFM images of TiO2 thin films, (a) Pure TiO2; (b) 1%Y:TiO2; (c) 2%Y:TiO2; (d) 3%Y:TiO2.

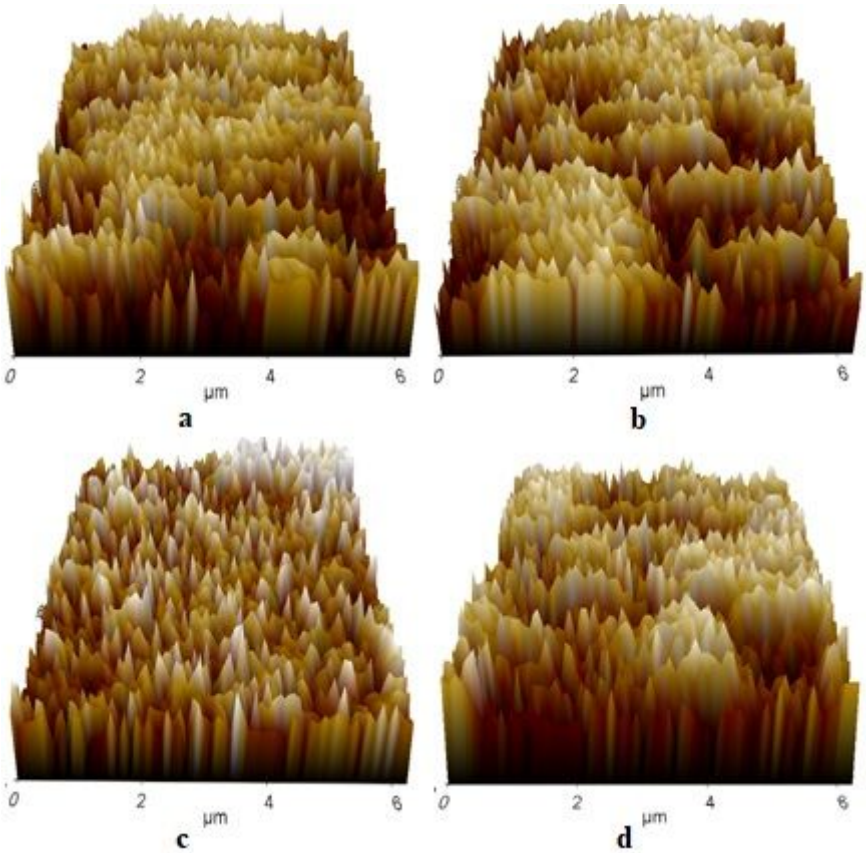

Figure 3

AFM images of TiO2 thin films, (a) Pure TiO2; (b) 1%Y:TiO2; (c) 2%Y:TiO2; (d) 3%Y:TiO2.

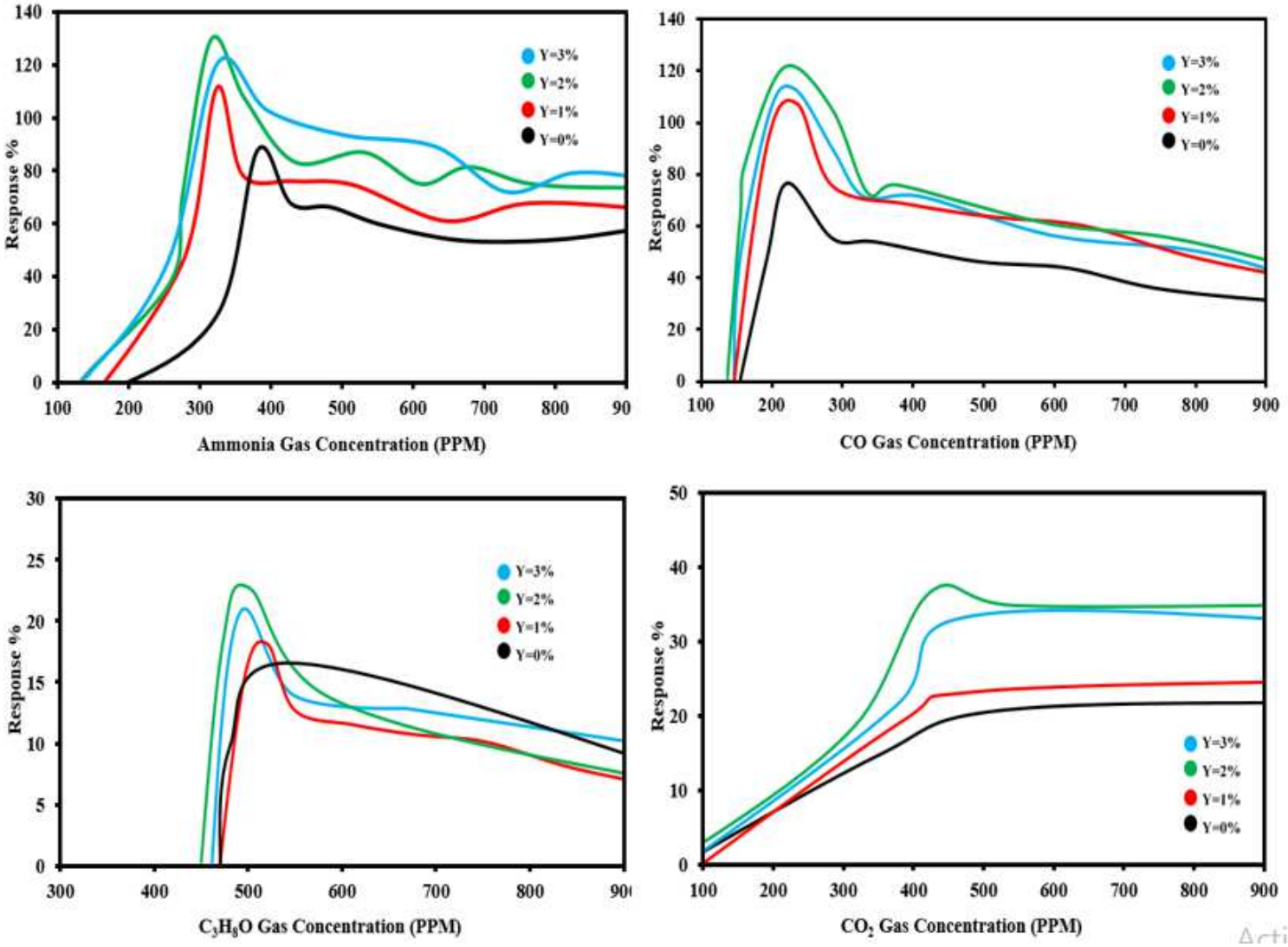

Figure 4

Response of different gases with different composition of thin films and concentrations of gases

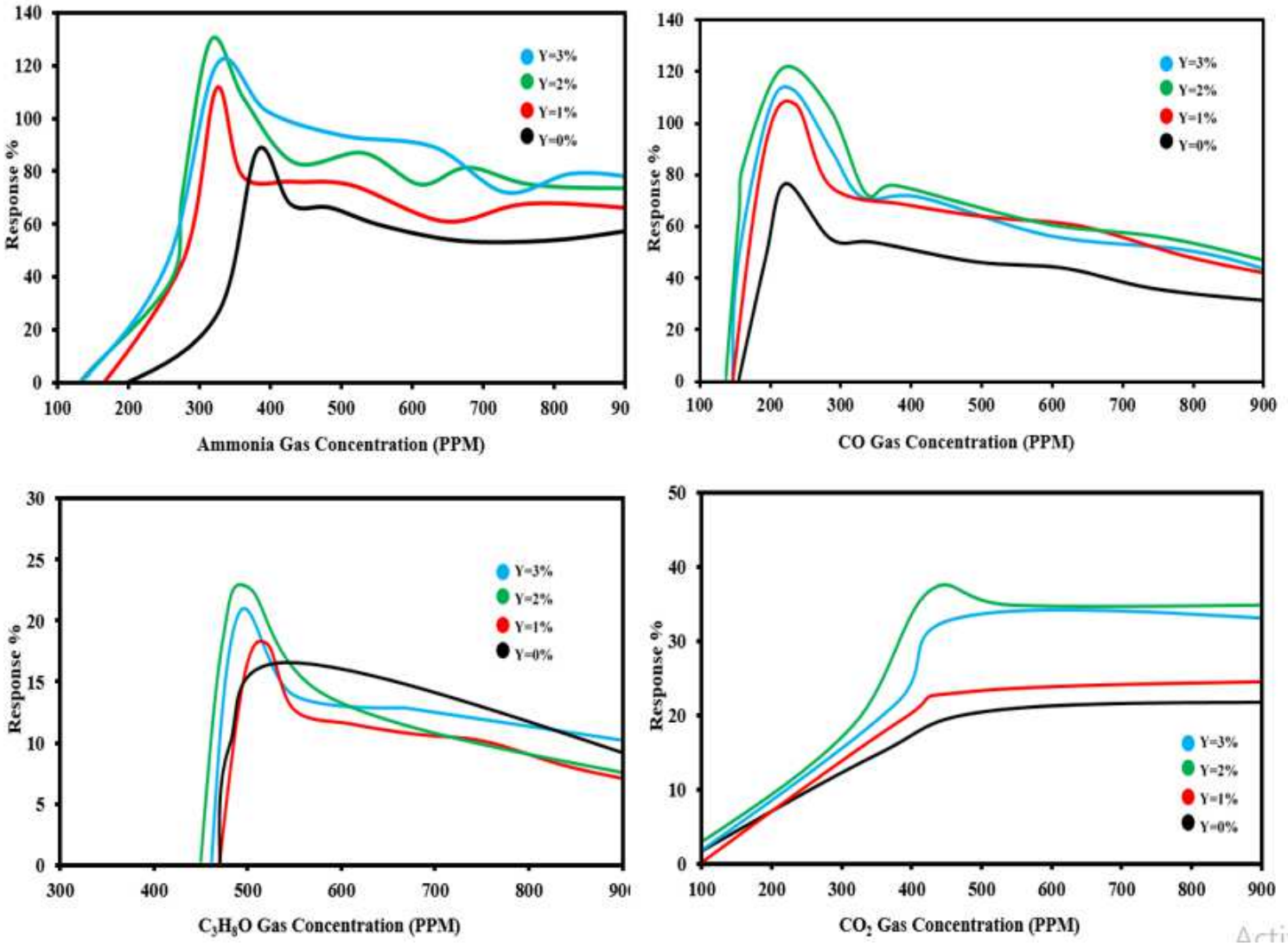

Figure 4

Response of different gases with different composition of thin films and concentrations of gases

Supplementary Files

This is a list of supplementary files associated with this preprint. Click to download.

- Fig.S1HomemadeSpinCoater.PNG
- Fig.S1HomemadeSpinCoater.PNG
- Fig.S2grainSizeDistributions.jpg
- Fig.S2grainSizeDistributions.jpg
- Fig.S3XPSanalysis.PNG
- Fig.S3XPSanalysis.PNG
- Fig.S4EDSSpectra.PNG

- Fig.S4EDSSpectra.PNG